Observation of a hole-size-dependent energy shift of the surface-plasmon resonance in Ni antidot thin films

H. Fang,[1] B. Caballero,[2] E. M. Akinoglu,[1] E. Th. Papaioannou,[3] A. García-Martín,[2] J. C. Cuevas,[4] M. Giersig,[1,5] and P. Fumagalli[1,a)]

[1]*Institut für Experimentalphysik, Freie Universität Berlin, 14195 Berlin, Germany*
[2]*IMM-Instituto de Microelectrónica de Madrid (CNM-CSIC), Isaac Newton 8, PTM, Tres Cantos, E-28760 Madrid, Spain*
[3]*Fachbereich Physik and Landesforschungszentrum OPTIMAS, Technische Universität Kaiserslautern, 67663 Kaiserslautern, Germany*
[4]*Departamento de Física Teórica de la Materia Condensada and Condensed Matter Physics Center (IFIMAC), Universidad Autónoma de Madrid, E-28049 Madrid, Spain*
[5]*Helmholtz Zentrum Berlin, Institute of Nanoarchitectures for Energy Conversion, 14195 Berlin, Germany*

A combined experimental and theoretical study of the magneto-optic properties of a series of nickel antidot thin films is presented. The hole diameter varies from 869 down to 636 nm, while the lattice periodicity is fixed at 920 nm. This results in an overall increase of the polar Kerr rotation with decreasing hole diameter due to the increasing surface coverage with nickel. In addition, at photon energies of 2.7 and 3.3 eV, where surface-plasmon excitations are expected, we observe distinct features in the polar Kerr rotation not present in continuous nickel films. The spectral position of the peaks exhibits a red shift with decreasing hole size. This is explained within the context of an effective medium theory by a change in the effective dielectric function of the Ni thin films. © 2015 AIP Publishing LLC. [http://dx.doi.org/10.1063/1.4917513]

Optical and magneto-optic (MO) properties of periodic ferromagnetic thin-film nanostructures have been studied intensively during the last years,[1–8] especially the effect of the surface-plasmon resonance (SPR) on the magneto-optic Kerr effect (MOKE). At the end of the 1990s, extraordinary optical transmission through a periodic array of sub-wavelength holes was observed and described as resonant excitation of a surface plasmon polariton (SPP).[9] As a result, a considerable amount of theoretical and experimental studies on the excitation of plasmons in noble metals has been carried out[10] motivated by the low absorption losses in metals and their potential applications. In particular, by changing the structural parameters of the array, it is possible to tailor the transmission properties at a desired wavelength. Later on, MO studies on pure plasmonic materials revealed a measurable MO activity if localized SPRs are excited under an extremely high applied magnetic field.[11] The MO response was found to be a consequence of an increase of the magnetic Lorentz force induced by the large collective movement of the conduction electrons in the nanostructures when the resonance is excited. By combining materials with ferromagnetic and plasmonic properties, the ferromagnet induces MO activity and the noble metal supports the excitation of weakly damped plasmons[12–14] increasing the electromagnetic field intensity inside the ferromagnet, and therefore, the MO response of the system. Additionally, in the case of pure ferromagnetic metals, the interaction of light with ferromagnetic nanoscale arrays of holes in an applied magnetic field leads to exciting optical

and magneto-optic properties.[4] Using different advanced fabrication techniques, one can design purely ferromagnetic patterned nanostructures such as grating[15] and dot/anti-dot structures[3,16,17] in uniform thin films.

In this work, ferromagnetic nickel antidot thin films are fabricated and the optical and MO properties are studied experimentally and theoretically by analyzing the dependence of the polar Kerr effect on the size of the nanostructures. The optical and MO response of the structures are obtained using the MOKE. For the simulations, a scattering matrix method (SMM)[18,19] was used. The aim is to correlate the MO response to the hole size and explain the origin of the tuning effect of the Kerr rotation.

Nanostructured Ni films were produced on Si (111) substrates with a native oxide layer using self-assembly sphere lithography (SSL). The details of the process are as follows.[20,21] Polystyrene (PS) spheres of 920 nm diameter were dispersed in an ethanol-water solution. The mixture was then slowly applied to the surface of milli-Q water in a Petri dish using a glass pipette. After formation of a hexagonal close-packed structure of the PS spheres on the water surface, a substrate was placed underneath. By slowly evaporating the water, the PS spheres deposited onto the substrate. Thereafter, the diameter of the spheres has been reduced in a controlled way by means of reactive ion etching in an oxygenated plasma atmosphere.[22] By increasing the etching time, the diameter of the sphere was reduced from 869 nm to 636 nm. These structures act as a lithography mask during physical vapor deposition. Deposition of 50 nm Ni was carried out in an e-beam evaporation system with a base pressure of 10^{-7} mbar. The spheres were thereafter dissolved by chemical treatment, leaving films with a regular pattern in form of a hexagonal array of circular holes on the substrates.

a)Author to whom correspondence should be addressed. Electronic mail: paul.fumagalli@fu-berlin.de. Phone: +49-30 838-54642. Fax: +49-30 838-454642.

106, 153104-1
© 2015 AIP Publishing LLC

The topography of the samples was characterized by scanning electron microscopy (SEM) as shown in Fig. 1(a).

The optical and MO properties of the films were investigated using a fully automated MOKE spectrometer in polar configuration, i.e., a magnetic field is applied perpendicular to the sample surface. S-polarized incident light is used at an incidence angle of ~3°. The Kerr rotation is measured by employing a lock-in technique in combination with a null method. It operates with a resolution of 2 mdeg in an energy range of 0.8–5 eV (248–1550 nm) and in an applied magnetic field of up to 1.6 T.[23] An aluminum mirror was applied as a reference in order to compensate for the influence of Faraday rotation from the optical components of the setup. To cancel out the influence of stress-induced birefringence effects, all measurements were taken in both magnetic field directions and subtracted from each other.

The reflectivity spectra were derived directly from the MOKE measurement without an extra measurement by using the parameters obtained from the null method. The values are normalized to the values of the aluminum mirror yielding a relative reflectivity.

In the simulations, we used a scattering matrix method (SMM) to calculate the optical and MO response of the structures. Details are published elsewhere.[18,19]

Figure 1(b) shows the relative-reflectivity spectra as derived from the MOKE measurement and the magneto-optic Kerr spectra of the Ni antidot thin films. In the relative-reflectivity spectra, we can see a structure originating from the Si substrate at 3.4 eV which is most prominent in the discontinuous samples forming island ($d = 869$ and 819 nm). Apart from the Si feature, minima are observed at around 2.7 eV (A) and 3.3 eV (B). As will be shown below, these minima are the result of a resonant coupling of light to surface-plasmon excitations at the interface of the Ni films.

In the magneto-optic Kerr spectra, the overall (negative) polar Kerr rotation increases with decreasing hole diameter. Since the inter-hole spacing or lattice constant is kept constant at 920 nm, this must directly be related to the change in hole size. By decreasing the hole diameter, the surface area of the MO active material is increased yielding a larger polar Kerr rotation. Focusing now on the spectral features, the MO response is completely different from that of a continuous Ni film. We find two distinct maxima of the absolute value of the (negative) polar Kerr rotation at approximately the same photon energy as the structures in the reflectivity spectra, i.e., around 2.7 eV (A) and 3.3 eV (B). Since the spectrum of a continuous Ni film is smooth, the structures must be related to the hole array. In addition, a red shift of the two peaks, i.e., a shift to lower photon energies with decreasing hole diameter, is clearly observed in the MOKE spectra. In the relative-reflectivity spectra, the shift can also be seen but it is less prominent.

In order to understand our experimental observations, calculations have been carried out for both the reflectivity and the polar Kerr rotation making use of a generalized scattering-matrix approach able to describe MO effects in
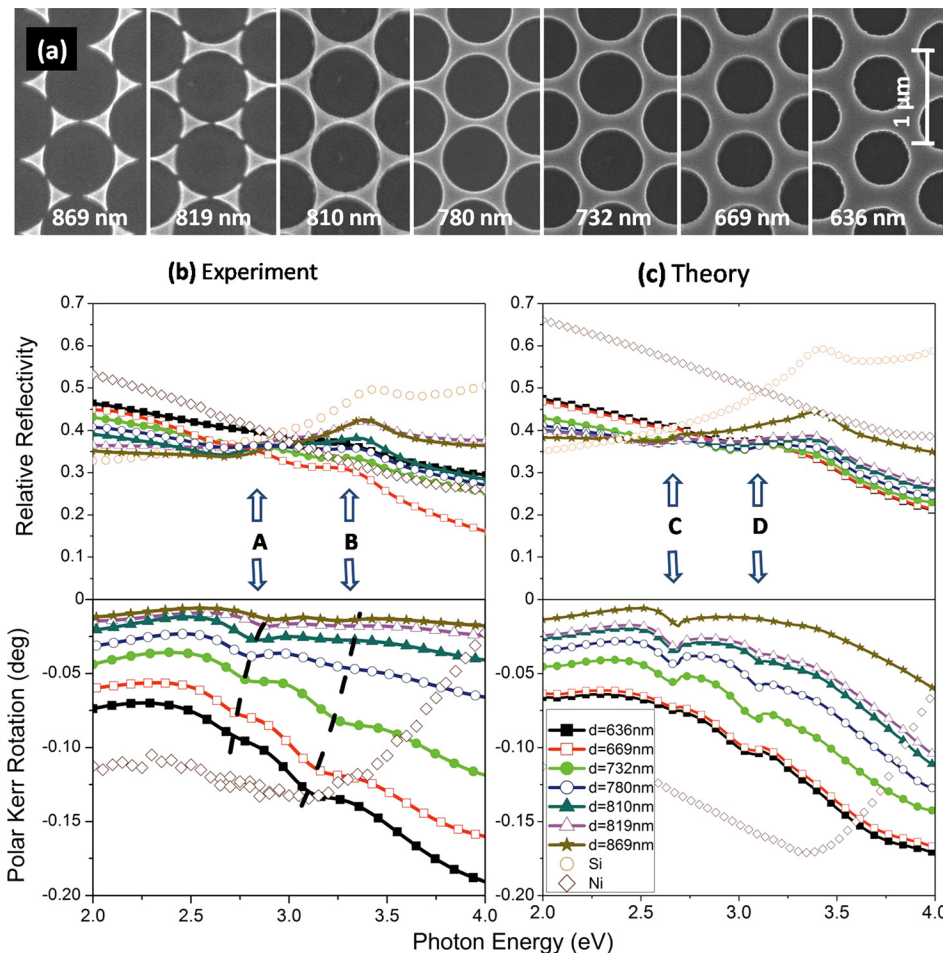

FIG. 1. (a) Scanning electron micrographs of a series of 50 nm thick Ni samples made by SSL. The lattice parameter a_0 of the hexagonal array is 920 nm, and the hole diameter varies from 869 down to 636 nm. (b) Measured relative reflectivity (top) and polar-Kerr rotation (bottom) for the series of Ni antidot samples. For comparison, the data of a continuous Ni film and Si substrate are included as well. The reflectivity is normalized to the reflectivity of an Al mirror. The position of the observed peaks is labeled *A* and *B* in the reflectivity and marked by dashed lines as a guide to the eye in the polar Kerr rotation. (c) Simulated reflectivity and polar Kerr rotation versus photon energy. *C* and *D* mark the position of the peaks.

periodically patterned systems.[18,19] The reflectivity minima and the maxima of the absolute value of (negative) polar Kerr rotation are related to the surface plasmon excitation at the metal/dielectric or the metal/air interface. It is well known that in a smooth metal surface a surface plasmon cannot be excited with light impinging from the air. To obtain a resonant excitation, one needs frequency and momentum matching between incoming light and surface plasmon. This is established by coupling of the surface plasmon to the lattice periodicity, the so-called Bragg plasmon.[1] In the case of a hexagonal lattice, the resonance for normal incidence can be written as

$$\lambda = \text{Re}\left(\frac{a_0}{\sqrt{\frac{4}{3}\left(i^2 + j^2 + ij\right)}} \sqrt{\frac{\varepsilon_m \varepsilon_d}{\varepsilon_m + \varepsilon_d}} \right). \tag{1}$$

Here, a_0 is the lattice constant of the periodic array and the integers i and j denote the order of the surface plasmon resonances. On the other hand, ε_m and ε_d are the dielectric constants of the metal and the dielectric, respectively. Using Eq. (1), one can easily check that the observed spectral position of the minima in the reflectivity data and of the maxima of the absolute value of the (negative) Kerr rotation are closely related to the energy corresponding to the second and the third order of the surface plasmon excitations at the air/nickel interface. Since in our case all samples are hexagonal lattices with the same lattice constant $a_0 = 920$ nm, no spectral shift is expected from Eq. (1).

In Fig. 1(c), the calculated spectra for the reflectivity and the polar Kerr rotation of the corresponding Ni antidot films are presented assuming normal incidence. The simulations are in fair qualitative agreement with the experimental results. The overall (negative) polar Kerr rotation increases when the hole size decreases. The energetic positions of the plasmon excitations (C and D), responsible for the structures, are similar in both reflectivity and Kerr spectra to that in the experimental data. The calculation evidences in addition a small kink close to the position of the plasmon excitation related to the Wood anomaly.[24] Because of its purely geometric origin in the periodicity of the lattice, the kink appears at the same photon energy for all samples and does not shift with decreasing hole diameter. However, the kink is not resolved in the experimental data, possibly due to insufficient resolution. For the kink to be observed, a large degree of perfection of the hole lattice is needed within the area of illumination. Small variations of the lattice parameter within the spot size of $\sim$5 mm^2 would wash it out.

The dependence of the MO response on the hole size, i.e., the energetic red shift of the maxima of the absolute value of the (negative) Kerr rotation with decreasing diameter, is clearly reproduced in the calculations. The dependence is most prominent in the structure at lower photon energy. To explain the experimentally observed red shift with hole diameter, we introduced in the calculations an effective medium approximation. Instead of using for ε_m, the dielectric constant of a continuous film of Ni, an effective dielectric constant proportional to the amount of Ni (membrane) and air (holes) has been applied in the following way:
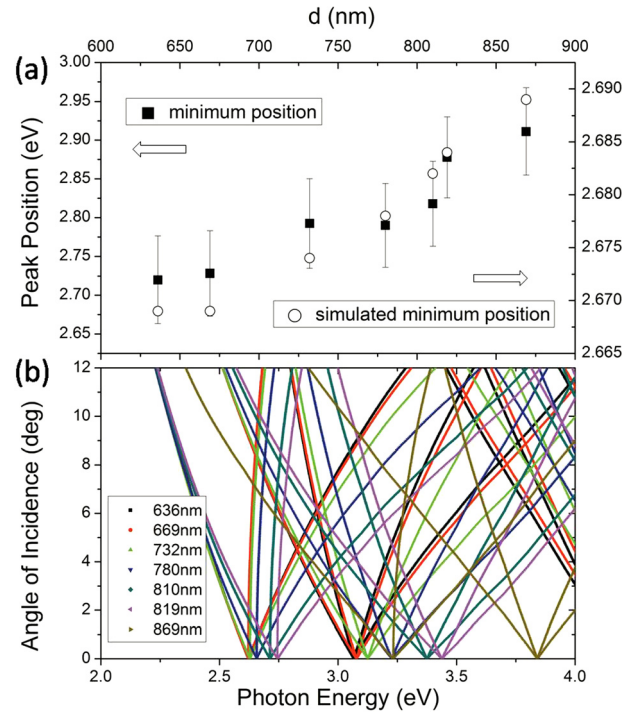

FIG. 2. (a) Photon energy of the first structure in the polar Kerr spectra as a function of hole diameter d as derived from experimental data (solid squares) and theory (open circles). Note the different scaling. (b) Calculated dispersion relation of the Bragg plasmons at the Ni/air interface as a function of angle of incidence for different hole diameters.

$$\varepsilon_m = f * \varepsilon_{Ni} + (1 - f) * \varepsilon_{air}, \tag{2}$$

where f is the area fraction of Ni at the surface. As a consequence, it will depend on the radius of each sample. To compare with experiment, the photon energy of the first peak is plotted in Fig. 2(a) as a function of hole size as derived from experiment (solid squares) and from calculation at normal incidence (open circles). Note the different scaling. The two curves are in fair agreement except for the size of the shift. The large error bars in the experimental data result mainly from the broadness of the structures. The broadening, and in part, the discrepancy in the size of the shift is due to the finite angle of incidence of $\sim$3° used in the MOKE set-up as explained by a detailed calculation of the dispersion relation of the Bragg plasmons shown in Fig. 2(b). For varying angle of incidence, it reveals an asymmetric splitting of the Bragg peaks. For an angle of incidence of 3°, the splitting amounts to $\sim$0.2 eV. Due to the limited photon-energy resolution of the MOKE spectrometer, the splitting is merely observed as an additional broadening of the peaks. This has been taken into account in the error bars. The asymmetry of the splitting, on the other hand, will increase the hole-size-dependent shift because the branching is larger on the high-energy side yielding a better agreement with experiment.

In conclusion, the optical and magneto-optic properties of Ni antidot films with fixed lattice periodicity but varying hole diameter were investigated. Pronounced maxima of the absolute value of the Kerr rotation were observed which can be related to surface plasmon resonances. Theoretical simulations are in good agreement with experimental results. Although keeping the lattice parameter of the array fixed, the position of the first minimum of the Kerr rotation is red shifted with

decreasing hole size. This dependence is qualitatively explained by introducing an effective metal dielectric constant due to an increasing Ni coverage at the surface when the hole diameter is decreasing. The broadening of the experimentally observed plasmon resonances is explained by the splitting of the Bragg peaks as a function of angle of incidence.

[1]G. Ctistis, E. Papaioannou, P. Patoka, J. Gutek, P. Fumagalli, and M. Giersig, Nano Lett. **9**(1), 1–6 (2009).

[2]E. T. Papaioannou, V. Kapaklis, E. Melander, B. Hjörvarsson, S. D. Pappas, P. Patoka, M. Giersig, P. Fumagalli, A. Garcia-Martin, and G. Ctistis, Opt. Express **19**(24), 23867–23877 (2011).

[3]J. F. Torrado, E. T. Papaioannou, G. Ctistis, P. Patoka, M. Giersig, G. Armelles, and A. Garcia-Martin, Phys. Status Solidi RRL **4**(10), 271–273 (2010).

[4]E. T. Papaioannou, V. Kapaklis, P. Patoka, M. Giersig, P. Fumagalli, A. Garcia-Martin, E. Ferreiro-Vila, and G. Ctistis, Phys. Rev. B **81**(5), 054424 (2010).

[5]J. B. Gonzalez-Diaz, A. Garcia-Martin, G. Armelles, D. Navas, M. Vazquez, K. Nielsch, R. B. Wehrspohn, and U. Gosele, Adv. Mater. **19**(18), 2643–2647 (2007).

[6]E. Melander, E. Ostman, J. Keller, J. Schmidt, E. T. Papaioannou, V. Kapaklis, U. B. Arnalds, B. Caballero, A. Garcia-Martin, J. C. Cuevas, and B. Hjorvarsson, Appl. Phys. Lett. **101**(6), 063107 (2012).

[7]A. A. Grunin, A. G. Zhdanov, A. A. Ezhov, E. A. Ganshina, and A. A. Fedyanin, Appl. Phys. Lett. **97**(26), 261908 (2010).

[8]D. Tripathy, P. Vavassori, and A. O. Adeyeye, J. Appl. Phys. **109**(7), 07B902 (2011).

[9]T. W. Ebbesen, H. Lezec, H. F. Ghaemi, T. Thio, and P. A. Wolff, Nature **391**(6668), 667–669 (1998).

[10]F. J. Garcia-Vidal, L. Martin-Moreno, T. Ebbesen, and L. Kuipers, Rev. Mod. Phys. **82**(1), 729 (2010).

[11]B. Sepulveda, J. B. Gonzalez-Diaz, A. Garcia-Martin, L. M. Lechuga, and G. Armelles, Phys. Rev. Lett. **104**(14), 147401 (2010).

[12]G. Armelles, A. Cebollada, A. Garcia-Martin, and M. U. Gonzalez, Adv. Opt. Mater. **1**(1), 10–35 (2013).

[13]G. X. Du, T. Mori, M. Suzuki, S. Saito, H. Fukuda, and M. Takahashi, J. Appl. Phys. **107**(9),09A928 (2010).

[14]S. Fan, Nat. Photonics **4**(2), 76–77 (2010).

[15]D. M. Newman, M. L. Wears, R. J. Matelon, and I. R. Hooper, J. Phys.: Condens. Matter **20**(34), 345230 (2008).

[16]N. Maccaferri, A. Berger, S. Bonetti, V. Bonanni, M. Kataja, Q. H. Qin, S. van Dijken, Z. Pirzadeh, A. Dmitriev, J. Nogués, J. Åkerman, and P. Vavassori, Phys. Rev. Lett. **111**(16), 167401 (2013).

[17]V. Bonanni, S. Bonetti, T. Pakizeh, Z. Pirzadeh, J. Chen, J. Nogués, P. Vavassori, R. Hillenbrand, J. Åkerman, and A. Dmitriev, Nano Lett. **11**(12), 5333–5338 (2011).

[18]A. García-Martín, G. Armelles, and S. Pereira, Phys. Rev. B **71**(20), 205116 (2005).

[19]B. Caballero, A. García-Martín, and J. C. Cuevas, Phys. Rev. B **85**(24), 245103 (2012).

[20]A. Kosiorek, W. Kandulski, P. Chudzinski, K. Kempa, and M. Giersig, Nano Lett. **4**(7), 1359–1363 (2004).

[21]E. M. Akinoglu, A. J. Morfa, and M. Giersig, Turk. J. Phys. **38**, 563–572 (2014).

[22]E. M. Akinoglu, A. J. Morfa, and M. Giersig, Langmuir **30**(41), 12354–12361 (2014).

[23]P. Fumagalli, Ph.D. thesis No. 9082, Swiss Federal Institute of Technology, 1990.

[24]R. W. Wood, Phys. Rev. **48**(12), 928–936 (1935).